Dilution of nematic surface potentials: Relaxation dynamics

André M. Sonnet
Dipartimento di Ingegneria Chimica, Università di Napoli Federico II, Piazzale Tecchio 80, I-80125 Napoli, Italy

Epifanio G. Virga
Dipartimento di Matematica, Istituto Nazionale di Fisica della Materia, Università di Pavia, Via Ferrata 1, I-27100 Pavia, Italy

Georges E. Durand
Laboratoire de Physique des Solides associé au CNRS (LA2), Université Paris Sud, F-91405 Orsay Cedex, France
(Received 18 February 2000)

Surface potentials can be regarded as diluted in space. By use of such a dilution model and Ericksen-Leslie theory we study the free relaxation of a nematic liquid crystal on an anchoring surface, after removal of an applied disorienting field. Depending on the initial distortions, we find either a relatively slow relaxation controlled by the bulk, or a fast relaxation characteristic of the anchoring surface. Comparing the dynamics described by the dilution model to one where the surface potential is localized, we estimate the surface viscosity in terms of the extension length of the surface torques.

PACS number(s): 61.30.−v, 68.10.Et

I. INTRODUCTION

A special class of nematic displays controlled by surface properties has recently been proposed [1] (for a review see [2]). These displays would be driven by the application of strong electric fields that could *break* the surface anchoring. The switching mechanism proposed to explain their behavior relies on the dynamics of the surface reorientation, starting when the field is suddenly turned off. Little is known about this surface dynamics. As an extension of the classical Rapini-Papoular balance of surface torques, which in statics describes the anchoring of the nematic director, Rapini has proposed a boundary condition that also includes a surface diffusion mechanism [3]. Such a time dependent boundary condition was already used in [4]. However, a systematic theory was only put forward later independently by Derzhanski and Petrov [5] and Kléman and Pikin [6]. This theory embodies the concept of surface viscosity. Several authors have since used this as a dynamical boundary condition [7–11].

In a previous paper [12] we attempted to illustrate the possible hydrodynamic origin of this phenomenological surface viscosity: to this end we adopted a mathematical model where the surface field responsible for the liquid crystal orientation is *diluted* in space over a thin anchoring layer; a similar dilution model had already been used in [13]. We further reconciled this model with the classical Rapini-Papoular model in statics [14]. In [12] we wrote the evolution equations for this problem according to Ericksen-Leslie theory [15] and made some conjectures concerning surface dynamics. In particular, we suggested the existence of a fast relaxation mode characteristic of the surface field.

In this paper we aim at solving the dynamical equations close to the boundary, resorting to both analytical and numerical methods. An interesting feature of this approach is that it does not rely on the dynamical Derzhanski-Petrov boundary condition; hence, knowing the solution of the evolution problem within our model, we are able to estimate the phenomenological surface viscosity. This is indeed the substantial difference between our theory for surface nematodynamics and those already proposed.

The paper is structured as follows. In Sec. II we recall how the Rapini-Papoular model has been extended by Derzhanski and Petrov to dynamics, and we address the problem of its compatibility with the evolution equation in the bulk. In Sec. III, we describe the dilution model for the surface field. Section IV is devoted to the analytic properties of the solution to the evolution equation within this model. Sections V and VI deal in detail with the two classes of relaxation problems already envisaged in [12]. In Sec. VII, we illustrate the relationship between the dilution and Derzhanski-Petrov models. Finally, in Sec. VIII we collect the conclusions to be drawn from our paper.

II. ORIENTATIONAL DYNAMICS

We briefly recall the equations that have so far been posited to describe statics and dynamics of nematic liquid crystals in the presence of a bounding surface. Consider a liquid crystal occupying the region $\mathcal{B}$ in space and subject to weak anchoring on the boundary $\partial\mathcal{B}$ of $\mathcal{B}$. The body is at equilibrium when the torque on the director $\mathbf{n}$ vanishes both in the bulk and on the bounding surface, that is, when

$$\mathbf{n}\times\mathbf{h}=\mathbf{0} \quad \text{in } \mathcal{B} \tag{1}$$

and

$$\mathbf{n}\times\mathbf{g}=\mathbf{0} \quad \text{on } \partial\mathcal{B}, \tag{2}$$

where $\mathbf{h}$ is commonly referred to as the *molecular field* and $\mathbf{g}$ is the *surface* molecular field introduced by analogy in [5]. Both $\mathbf{h}$ and $\mathbf{g}$ are computed from a variation of the nematic total free energy, including both volume and surface integrals. Letting $W=W(\mathbf{n},\nabla\mathbf{n})$ and $W_s=W_s(\mathbf{n})$ be the volume and surface free energy densities, one finds

$$\mathbf{h}=\mathrm{div}\left(\frac{\partial W}{\partial \nabla \mathbf{n}}\right)-\frac{\partial W}{\partial \mathbf{n}} \quad \text{in } \mathcal{B} \tag{3}$$

and

$$\mathbf{g}=-\frac{\partial W_s}{\partial \mathbf{n}}-\frac{\partial W}{\partial \nabla \mathbf{n}}\boldsymbol{\nu} \quad \text{on } \partial\mathcal{B}, \tag{4}$$

where $\boldsymbol{\nu}$ is the outer unit normal to $\partial\mathcal{B}$.

If the liquid crystal is not at equilibrium, these fields are not aligned along the director: they induce elastic torques which are balanced by the viscous torques. For simplicity, we assume in the following that neither flow nor backflow is present, and so the energy $\mathcal{D}$ dissipated per unit volume is given by

$$\mathcal{D}=\gamma_1\dot{\mathbf{n}}^2, \tag{5}$$

where γ_1 is the *rotational viscosity* [16,17], and a superimposed dot denotes the material time derivative. The dynamical counterpart of Eq. (1) is

$$\mathbf{n}\times\left(\mathbf{h}-\frac{1}{2}\frac{\partial \mathcal{D}}{\partial \dot{\mathbf{n}}}\right)=\mathbf{0} \quad \text{in } \mathcal{B}. \tag{6}$$

The need for a similar balance of torques on the surface also was felt rather early [3–6], and various attempts have also been made to measure the corresponding viscosity (see, e.g., [18]). It seems natural to introduce a dissipation function $\mathcal{D}_s$ for the surface; the simplest expression for an isotropic surface would be

$$\mathcal{D}_s=\gamma_s\dot{\mathbf{n}}^2, \tag{7}$$

where $\gamma_s=\gamma_1 l$ is the *surface viscosity* and l is a surface length. Recently, a more general expression for $\mathcal{D}_s$ that also takes into account surface anisotropy has been used [9]. In this setting, the dynamical counterpart of Eq. (2) proposed by Derzhanski and Petrov [5] is

$$\mathbf{n}\times\left(\mathbf{g}-\frac{1}{2}\frac{\partial \mathcal{D}_s}{\partial \dot{\mathbf{n}}}\right)=\mathbf{0} \quad \text{on } \partial\mathcal{B}. \tag{8}$$

Without a diffusive process on the surface, it is indeed possible to construct initial conditions for the director such that its incipient rotational velocity at the boundary gets arbitrarily large: it suffices to make the surface torque unbalanced at the initial time to induce a jump of $\mathbf{n}$ at the surface in the incipient dynamics. The introduction of a surface viscosity in the way just recalled has, however, one serious problem: since both Eqs. (6) and (8) specify the time derivative of the director on the boundary, a compatibility condition arises. This is not peculiar to nematodynamics, nor to ordinary hydrodynamics: it simply stems from imaging a relaxation mechanism that involves the same time derivative on the boundary as in the bulk. As a consequence, Eqs. (6) and (8) do not generally allow a description of the director relaxation after the removal of an external field (see Sec. VII for a detailed example of incompatibility and also for a way to take care of it).

In principle, a way to avoid this incompatibility would be not to neglect molecular inertia, thereby introducing a second time derivative of $\mathbf{n}$ in the bulk equation. We take a different path here because molecular inertia would bring in a molecular length smaller than l: we continue to neglect inertia and accordingly abandon the idea of a localized surface dissipation. This is the reason why we adopt the dilution model described below.

III. DILUTION MODEL

As remarked in the preceding section, describing the surface anchoring through the Derzhanski-Petrov boundary condition in general prevents a proper treatment of surface dynamics. Here we resort to a model that circumvents any incompatibility that this condition may cause.

To illustrate this model, we consider a liquid crystal in one space dimension with the anchoring on a single supporting wall competing against an external electric field. We assume the cell to be semi-infinite and restrict the director to a plane perpendicular to the wall. Since here only splay and bend deformations are relevant, the elastic contribution to the free energy density W_{def} can be written by using the one-constant approximation to the Oseen-Frank elastic free energy density:

$$W_{\mathrm{def}}=\frac{K}{2}(\nabla \mathbf{n})^2=\frac{K}{2}(\vartheta')^2, \tag{9}$$

where K is an average elastic modulus, ϑ is the angle that the director makes with the bounding plate, and a prime denotes differentiation with respect to the distance z from the plate. The density of the electric energy W_{ele} is given in SI units by

$$W_{\mathrm{ele}}=\tfrac{1}{2}\varepsilon_0\varepsilon_a E^2\sin^2(\vartheta-\vartheta_e), \tag{10}$$

where ε_0 is the dielectric constant of vacuum, $\varepsilon_a>0$ is the relative dielectric anisotropy, E is the strength of the electric field, and ϑ_e defines the direction along which it is applied. For simplicity, the electric field is assumed to be uniform throughout the cell and, in most of the paper, orthogonal to the plate ($\vartheta_e=\pi/2$).

In the dilution model, no singular surface energy W_s is defined on the bounding plate. The action of the surface is rather carried by a further bulk term, which describes how the surface torques decay with the distance from the wall:

$$\mathcal{W}_d:=\frac{1}{2}\int_0^\infty D(z)\sin^2\vartheta\, dz, \tag{11}$$

where $D(z)$ is the strength of the surface potential at the point with coordinate z. The anchoring described by Eq. (11) is planar, that is, the preferred surface alignment is parallel to the plate. It is convenient to define a total strength A of the anchoring by

$$A:=\int_0^\infty D(z)dz \tag{12}$$

and a characteristic dilution length by

$$h:=\frac{\int_0^\infty zD(z)dz}{\int_0^\infty D(z)dz}. \tag{13}$$

With these definitions the surface energy is rewritten as

$$\mathcal{W}_d = \frac{A}{2h}\int_0^\infty d(z)\sin^2\vartheta(z)dz, \tag{14}$$

where now

$$d(z) := \frac{h}{A}D(z) \tag{15}$$

is a dimensionless dilution function that is normalized to $\int_0^\infty d(z)dz = h$. We consider only weak anchoring, which is characterized by the inequality $h \ll L$ where

$$L := K/A. \tag{16}$$

It was found in [14] that in this case L can be interpreted as the usual surface extrapolation length.

With the potential in Eq. (11), the time evolution for the nematic orientation is governed by the equation

$$\tau_s\dot{\vartheta} = \xi_s^2\vartheta'' - \frac{1}{2}\left(d - \frac{\xi_s^2}{\xi_e^2}\right)\sin 2\vartheta. \tag{17}$$

Here the surface length

$$\xi_s := \sqrt{Kh/A} = \sqrt{Lh} \tag{18}$$

and the surface time

$$\tau_s := \frac{\gamma_1}{K}\xi_s^2 \tag{19}$$

have been introduced, along with the electric coherence length

$$\xi_e := \frac{1}{E}\sqrt{K/\varepsilon_0\varepsilon_a}. \tag{20}$$

Equation (17) is subject to the boundary condition

$$\vartheta' = 0 \quad \text{at } z = 0 \quad \text{for all } t \geqslant 0. \tag{21}$$

This reflects the fact that no localized torque is transmitted at the boundary. Unlike Eq. (8), this does not entrain any compatibility condition. For the typical values $L = 100\,\text{nm}$, $h = 10\,\text{nm}$, $K = 10^{-11}\,\text{N}$, and $\gamma_1 = 10^{-2}\,\text{kg m}^{-1}\,\text{s}^{-1}$, it turns out that $\tau_s = 1\,\mu\text{s}$.

Essentially, the relaxation problem we study exhibits a competition between the surface orientation, which will evolve fast, and the bulk orientation, which will drag behind and hamper it. In the following sections we strive to make this intuitive description precise.

IV. PROPERTIES OF SOLUTIONS

No solution in closed form is available for Eq. (17) even for simple choices of the dilution function d. A simpler version of Eq. (17) is indeed the Fisher-Kolmogorov equation. To tackle this problem, we pursue a twofold approach. Information about the incipient dynamics can be gained by a linearization about the initial data. For the dynamics at later times, we resort to a numerical solution of Eq. (17) with special choices for the dilution potential and viscosity.

Because here the surface effects are diluted in space, the orientation at $z = 0$ is not necessarily the best measure of the surface evolution. Instead, for a function v, we introduce a localized norm defined by

$$\|v\|_2 := \sqrt{(1/h)\int_0^h v^2 dz}, \tag{22}$$

which expresses an average of v over the shortest meaningful length near the surface.

To evaluate the speed of the director reorientation when the initial condition is represented by the function $\varphi = \varphi(z)$, we define

$$u(z,t) := \vartheta(z,t) - \varphi(z). \tag{23}$$

It readily follows from Eq. (17) that close to the initial time u obeys the linearized equation

$$\tau_s\dot{u} = \xi_s^2 u'' - fu + g, \tag{24}$$

where

$$f := d\cos\varphi \tag{25}$$

and

$$g := \xi_s^2\varphi'' - \tfrac{1}{2}\,d\sin 2\varphi. \tag{26}$$

The surface relaxation is represented by the time evolution of $\|u\|_2$. The following estimate for the first derivative of $\|u\|_2$ is obtained by use of Schwarz's inequality:

$$\frac{d}{dt}\|u\|_2 = \frac{\int_0^h u\dot{u}\,dz}{\sqrt{h\int_0^h u^2 dz}} \leqslant \|\dot{u}\|_2. \tag{27}$$

Since $u \equiv 0$ at $t = 0$, from both Eqs. (24) and (27) an upper bound for the initial speed of the surface relaxation easily follows:

$$\frac{d}{dt}\|u\|_2(0) \leqslant \frac{1}{\tau_s}\|g\|_2. \tag{28}$$

Moreover, as long as u obeys the condition

$$uu'|_{z=h} < 0, \tag{29}$$

a finer estimate can be derived from an extension of the Wirtinger inequality [19]: for t sufficiently small

$$\|u\|_2 \leqslant \frac{\|g\|_2}{\xi_s^2\gamma_0^2/h^2 - \|f\|_\infty}\left(1 - e^{-\xi_s^2\gamma_0^2/h^2 - \|f\|_\infty t/\tau_s}\right), \tag{30}$$

where $\|f\|_\infty$ is the supremum of $|f|$ in $[0,h]$ and γ_0 is the smallest root of the equation

$$-\gamma_0\tan\gamma_0 = \frac{hg'(h)}{g(h)}. \tag{31}$$

In this way, besides the speed of the incipient relaxation, we can also estimate the time scale over which this takes place.

In the following we study the relaxation from two classes of initial director configurations: namely, equilibrium profiles generated by a finite electric field and totally flat profiles. We devote two distinct sections to the analysis of these different relaxation processes: we shall see that one is slow, while the other is fast.

V. SLOW DYNAMICS

Here we discuss the free relaxation of an equilibrium profile after the removal of the electric field that has produced it. We first consider the case where the electric field is above the saturation value. The orientation ϑ is then uniform at the beginning, $\vartheta \equiv \pi/2$. Switching off the field changes a stable equilibrium into an unstable one, but it does not prompt any relaxation, in the absence of either external perturbations or thermal fluctuations. This problem exceeds the scope of the present paper.

We now focus attention on the case where the field is below the saturation value. The corresponding equilibrium profiles have been treated in a previous work [14]. Without solving the dynamic equation, an estimate for the time scale of the incipient evolution can be obtained from the static solution. Since φ is at equilibrium in the presence of the field, by Eq. (17), it obeys the equation

$$\xi_s^2 \varphi'' = \frac{1}{2}\left(d - \frac{\xi_s^2}{\xi_e^2} \right) \sin 2\varphi. \tag{32}$$

Thus, at the instant when the electric field is switched off, by Eq. (26),

$$g = \xi_s^2 \varphi'' - \frac{d}{2} \sin 2\varphi = \frac{\xi_s^2}{2\xi_e^2} \sin 2\varphi \leqslant \frac{\xi_s^2}{2\xi_e^2}. \tag{33}$$

This upper bound for g is attained for $\varphi = \pi/4$, which, for a surface anchoring sufficiently strong, is a value actually taken by the initial profile near the boundary. By Eq. (28), the fastest possible time is thus

$$\tau_s \frac{2\xi_e^2}{\xi_s^2} = 2\,\frac{\gamma_1}{K}\,\xi_e^2 = 2\,\tau_e\,, \tag{34}$$

where the electric relaxation time τ_e is defined as

$$\tau_e := \frac{\gamma_1}{K}\,\xi_e^2. \tag{35}$$

It follows from Eq. (17) that after the removal of the field the evolution of ϑ is governed by

$$\tau_s \dot{\vartheta} = \xi_s^2 \vartheta'' - \tfrac{1}{2}\, d \sin 2\vartheta. \tag{36}$$

At later times, the surface angle will approach zero and its evolution will become even slower while the profile keeps diffusing in the bulk.

This picture is confirmed by numerical solutions of Eq. (36) subject to Eq. (21) for a number of initial conditions. It is expedient to introduce the subsurface relaxation time τ_h defined as

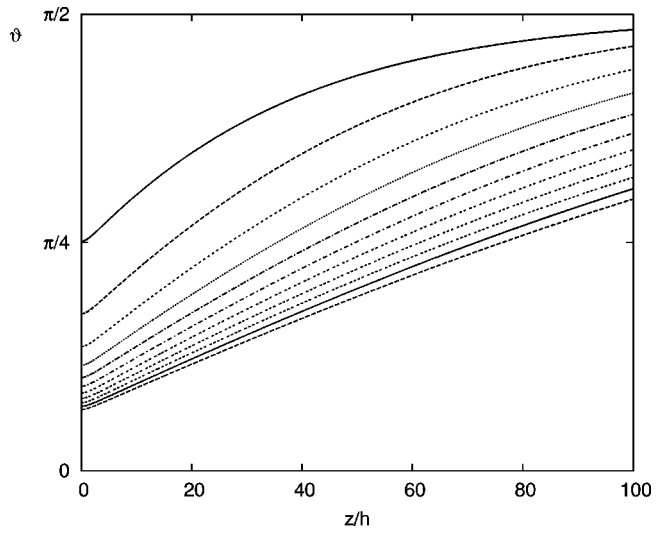

FIG. 1. Typical evolution starting from an equilibrium profile produced by a field with coherence length $\xi_e = 36h$. Two adjacent profiles differ in time by $1000\tau_h$.

$$\tau_h := \frac{\gamma_1}{K} h^2; \tag{37}$$

by comparing this to Eq. (19), one sees that τ_h is shorter than the surface time τ_s by the ratio h^2/ξ_s^2. Since τ_s is already in the range of microseconds, τ_h could then be a much shorter time.

For the numerical solution we chose $d(z) = \exp(-z/h)$ and we made Eq. (17) dimensionless by normalizing the length to h and the time to τ_h. To work on a finite space interval, we used the transformation $\tilde{z} = 1 - (1+z)^{-1/p}$ with $p = 3$. The resulting grid automatically has the feature that the interesting region close to the boundary is more finely resolved. We used a finite difference scheme with a semiimplicit time discretization of the Crank-Nicolson type and 1000 points for the space grid. The examples below were obtained with $\xi_s = 5h$ and accordingly $L = 25h$. The electric field was chosen such that the angle ϑ_0 that describes the director orientation at the surface satisfies $\vartheta_0 \approx \pi/4$ at equilibrium. We took $\xi_e = 36h$; it was proved in [14] that $\sin \vartheta_0 = L/\xi_e$ for $h \ll L$.

Qualitatively, Fig. 1 shows the typical surface relaxation of the orientation accompanied by a diffusion in the bulk of the rotational velocity $\dot{\vartheta}$. The characteristic time of this evolution is τ_e, and so it depends on the field that has produced the initial equilibrium profile (see also [12]): this time is larger than τ_s, but is still shorter than the relaxation time associated with a typical Fréedericksz transition. In practice, τ_e could be 10 μs for a 10 V/μm voltage applied across a cell with Fréedericksz transition at 1 V/μm.

At early times the relaxation takes place as if an effective field were slowly reduced in time with an effective coherence length $\hat{\xi}_e(z,t)$. This length is defined by pretending that ϑ is a solution to Eq. (32) with $\hat{\xi}_e$ instead of ξ_e. By comparing this equation and Eq. (36) we readily arrive at

$$\frac{\xi_e^2}{\hat{\xi}_e^2(z,t)} = -\frac{2\,\tau_e \dot{\vartheta}}{\sin 2\vartheta}. \tag{38}$$

Initially $\hat{\xi}_e = \xi_e$, and an estimate for the incipient dynamics easily follows from Eq. (38):

$$\tan\vartheta = \tan\vartheta|_{t=0} e^{-t/\tau_e} \quad \text{for } t \to 0^+. \tag{39}$$

At later times, $\hat{\xi}_e$ and ξ_e start to differ from one another at the surface, because the rotational velocity decreases close to the surface, while it diffuses into the bulk. We call this evolution adiabatic, as it can be regarded as a sequence in time of equilibrium profiles. All these results confirm the conjecture already made in [12]: although the surface alone could intrinsically relax faster, it is slowed down by the orientation curvature needed to match the bulk profile.

VI. FAST DYNAMICS

The adiabatic dynamics does not reveal the short time τ_s associated with the full strength of the surface field, just because close to equilibrium it is almost balanced by the curvature density ϑ'' concentrated within the dilution length. The memory of the field, kept in the bulk curvature over a characteristic length ξ_e, relaxes with rate τ_e^{-1}.

Higher rotational velocities can be expected when the initial profile is flat. As above, we discard the case $\vartheta \equiv \pi/2$ because its relaxation can be driven only by fluctuations. We can imagine, for instance, applying a sufficiently strong shear that produces the profile $\vartheta \equiv \vartheta_0 < \pi/2$ from the one obtained by an electric field above saturation. We study here the relaxation dynamics after the instantaneous removal of both shear and field.

In [12] it was conjectured that for such an initial profile the subsequent dynamics consists of two parts: In the first one, the flat profile builds up curvature density ϑ'' close to the boundary during the short time τ_s; in the second one, an adiabatic evolution takes place as above with a longer time $\tau_L := (L/h)\tau_s$. The characteristic time of the incipient relaxation can indeed be estimated as τ_s from Eq. (36), which at the initial time and for $z=0$ gives $2\tau_s \dot{\vartheta} = d(0)\sin 2\vartheta_0$.

A finer description of the incipient dynamics is delivered by the following argument. We take again $d(z) = \exp(-z/h)$ and explore the consequences of inequality (30) when $\varphi \equiv \vartheta_0$. We first note that the right-hand side of Eq. (31) is -1 for all ϑ_0, and so $\gamma_0 \approx 0.86$. Then we write Eq. (30) in a shorter form:

$$\|u\|_2 \leqslant a_0(1 - e^{-t/\tau_0}) \tag{40}$$

and, for $h \ll L$, we estimate both the amplitude a_0 and the relaxation time τ_0 as

$$a_0 \approx \frac{1}{3}\sin 2\varphi_0 \frac{h^2}{\xi_s^2 \gamma_0^2}, \qquad \tau_0 \approx \tau_s \frac{h^2}{\xi_s^2 \gamma_0^2} \approx \tau_h. \tag{41}$$

We thus expect a fast incipient increase of $\|u\|_2$.

As an example, we calculate the evolution starting from the constant profile $\vartheta_0 = \pi/4$ with the same values of the parameters as in Sec. V. In Fig. 2 we plot five profiles in the evolution for $0 < t \leqslant \tau_h$. At first, the profile tends to adjust itself to the shape of the exponential dilution function that determines the initial angular velocity. This induces a negative curvature everywhere, except close to the boundary where ϑ' has to vanish. This requirement creates a positive curvature density $\vartheta'' > 0$.

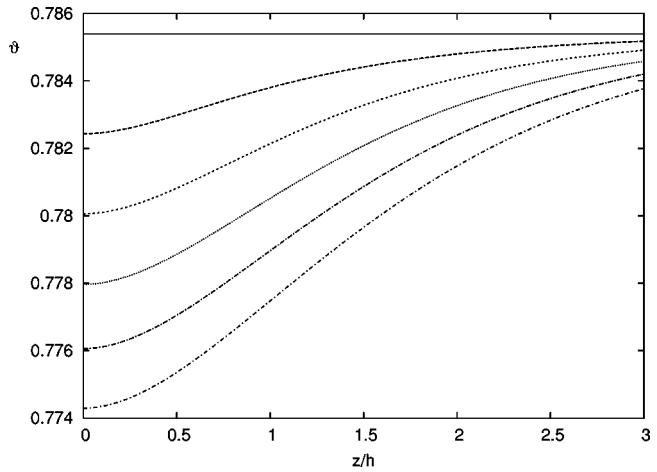

FIG. 2. Evolution starting from the constant profile $\vartheta \equiv \pi/4$. Two adjacent profiles differ in time by $0.2\tau_h$. The initial reorientation builds up curvature that compensates the surface torque; then the evolution becomes slower.

The accuracy of the estimate in Eq. (40) is shown in Fig. 3, where the actual evolution of $\|u\|_2$ computed numerically is compared to the exponential bound in Eq. (40). The right-hand side of Eq. (30) actually represents an *osculating* exponential to $\|u\|_2$ at $t=0$.

All this concerns incipient dynamics. To show the evolution at later times, we plot in Fig. 4 the function

$$v_{\text{eff}}(t) := \left.\frac{2\tau_s \dot{\vartheta}}{\sin 2\vartheta}\right|_{z=0}. \tag{42}$$

It can be regarded as an effective rotational velocity. A whole distribution of relaxation times is found in its decay, which reflects the fact that a finite surface energy is dissipated over a region ever penetrating the bulk, leading to a slower and slower process.

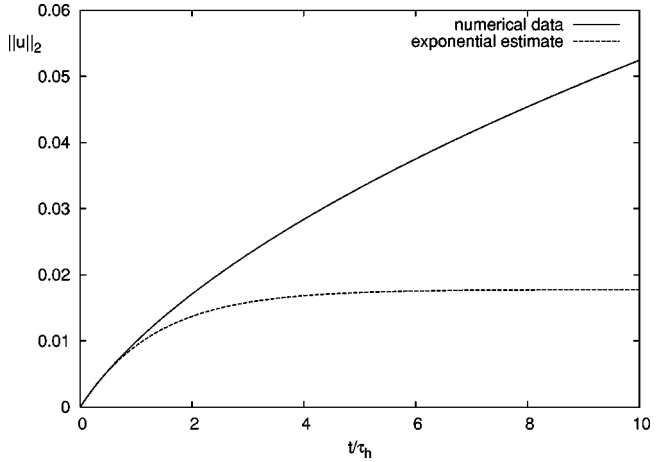

FIG. 3. The evolution of the difference norm in the incipient dynamics. The osculating exponential at $t=0$ shows the shortest relaxation time.

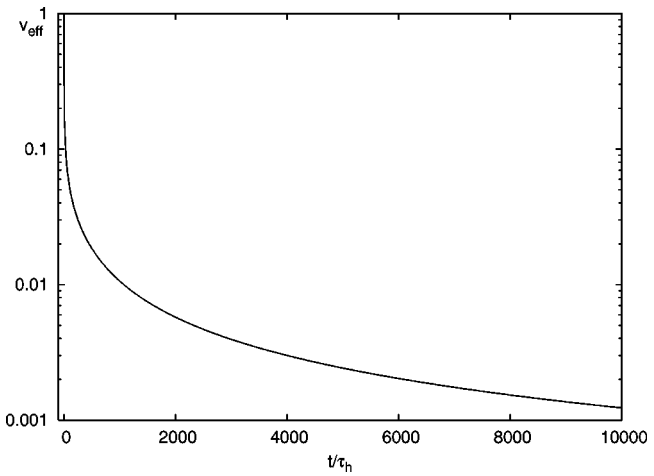

FIG. 4. Effective rotational velocity at $z=0$ as a measure of the surface rotational velocity. No fixed time scale can be identified; the surface dynamics becomes slower as the diffusion proceeds into the bulk.

To make our discussion more quantitative, we define at each time t_0 an amplitude $|A(t_0)|$ and a relaxation rate $r(t_0)$ by requiring that the exponential

$$A(t_0)e^{-r(t_0)(t-t_0)}+B \tag{43}$$

be osculating the graph of the function $a(t):=\|u\|_2$ at $t=t_0$. An easy computation gives

$$r(t_0)=-\left.\frac{\ddot{a}}{\dot{a}}\right|_{t=t_0} \quad \text{and} \quad A(t_0)=\left.\frac{\dot{a}^2}{\ddot{a}}\right|_{t=t_0}. \tag{44}$$

In Fig. 5 we plot $|A|$ against r using $t_0\in[0,10^3\tau_s]$ as a parameter for the same evolutions shown in Figs. 1 and 2. For the fast relaxation, the maximum amplitude actually appears for $r^{-1}\approx 8.5\tau_s$ at the time $t_0\approx 6\tau_s$. Indeed, τ_s would be the relaxation time of an isolated layer with thickness h in the absence of bulk. The relaxation rate with maximum amplitude is here reminiscent of this pure surface relaxation mode: it conveys through h information on the internal structure of the surface. For the slow relaxation, the amplitude attains its maximum at $t_0=0$; initially the relaxation time is $2\tau_e$ and then it slightly decreases toward τ_L while the memory of the field fades away.

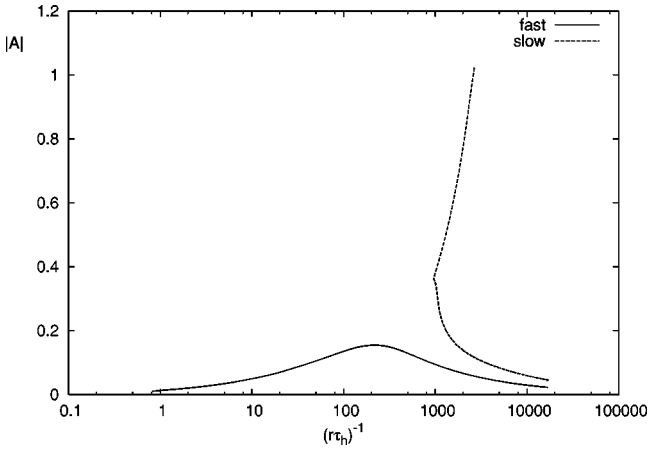

FIG. 5. Osculating exponentials. Parametric plots of the amplitude versus the dimensionless relaxation rate for both fast and slow dynamics.

VII. CLASSICAL SURFACE VISCOSITY

In Sec. II we discarded the Derzhanski-Petrov boundary condition (8) because it is not generally consistent with the evolution equation in the bulk. Nevertheless, it has been adopted by many authors as it conveys the idea that the balance of surface torques contains the essence of surface dynamics [9,11]. Here we show that this idea can indeed be given a precise meaning by interpreting the Derzhanski-Petrov boundary condition within the dilution model.

We adjust the director profile near the boundary so that it complies with the Derzhanski-Petrov condition at the initial time: no discontinuity thus arises on the boundary at all times, although the profile evolution is different. By comparing the evolution that obeys the Derzhanski-Petrov condition and that predicted by the dilution model, we can appreciate how they depart from one another in time. Since γ_s in Eq. (7) is a phenomenological parameter, choosing it so as to minimize this departure offers a means to relate the surface length l and the dilution length h.

We now illustrate by example both the incompatibility arising from the Derzhanski-Petrov boundary condition and our strategy to remedy it. In the same setting employed in Sec. III, the dynamic equation in the bulk takes the general form

$$\gamma_1\dot{\vartheta}=K\vartheta''+F(E,\vartheta), \tag{45}$$

where ϑ is the angle that the director makes with the bounding plate, K is the elastic modulus, and F is a function that describes the action of an external field with strength E. F vanishes whenever E does; it is easily seen that Eq. (17) is a special case of Eq. (45). Let now $\vartheta_0(t):=\vartheta|_{z=0}$ denote the director orientation at the surface. The typical Rapini-Papoular surface energy density W_s is given by

$$W_s=\frac{A}{2}\sin^2\vartheta_0, \tag{46}$$

where A is the strength of the anchoring. The dynamic boundary condition obtained from Eq. (8) with Eq. (7) then reads as

$$\frac{\gamma_1 l}{K}\dot{\vartheta}_0=\vartheta'|_{z=0}-\frac{1}{2L}\sin 2\vartheta_0, \tag{47}$$

where L is defined as in Eq. (16).

At equilibrium, the left-hand sides of both Eq. (45) and Eq. (47) vanish. When the field is abruptly switched off, F undergoes a jump, and according to Eq. (45) $\dot{\vartheta}\neq 0$. Since, however, at the initial time the director profile is unchanged, Eq. (47), which does not depend on the field, still requires $\dot{\vartheta}_0=0$, and so Eqs. (45) and (47) fail to be compatible at the very beginning.

This incompatibility can be removed by adjusting the initial director profile. To this end we change both the slope and the curvature of the initial profile close to the boundary so

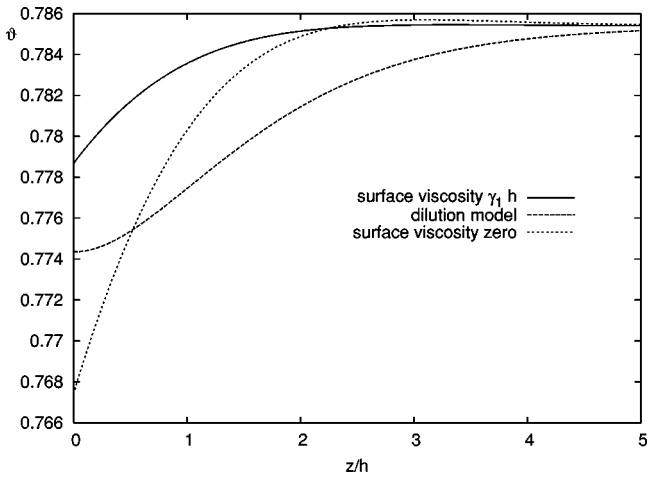

FIG. 6. Snapshots at $t=\tau_h$ from the evolution of the adapted and nonadapted profiles. The initial nonadapted profile is $\vartheta\equiv\pi/4$; it is adapted to surface viscosities with $l=0$ and h.

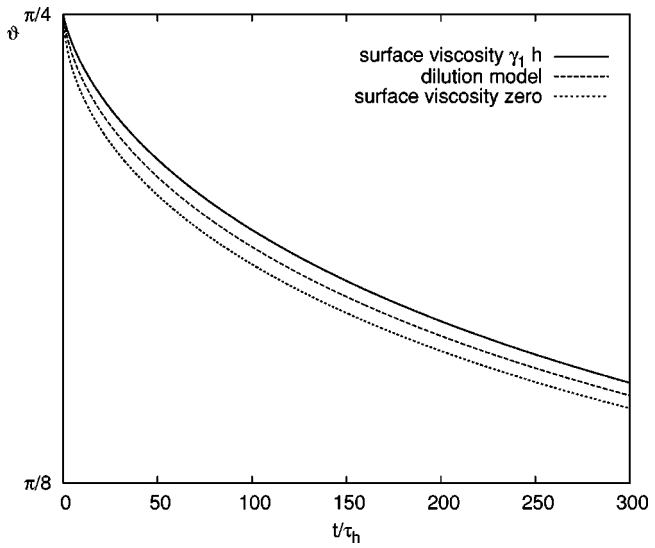

FIG. 7. Comparison of the surface orientation for the evolution of adapted and nonadapted profiles. The initial nonadapted profile is $\vartheta\equiv\pi/4$; it is adapted to surface viscosities with $l=0$ and h. The surface evolution predicted by the dilution model can be mimicked by a surface viscosity falling between 0 and $\gamma_1 h$.

that the bulk and surface rotational velocities match. We perform a local adaptation that affects the function $\varphi(z) := \vartheta|_{t=0}$ over a length ξ underneath the surface $z=0$. Formally, we replace φ by

$$\varphi_\alpha(z) := (1+\alpha z e^{-z/\xi})\varphi(z). \tag{48}$$

Clearly, $\varphi_\alpha(0)=\varphi(0)$, and, since $\varphi'(0)=0$,

$$\varphi'_\alpha(0)=\alpha\varphi(0) \quad \text{and} \quad \varphi''_a(0)=-\frac{2\alpha}{\xi}\varphi(0)+\varphi''(0). \tag{49}$$

On the other hand, when E vanishes, φ_α causes both Eqs. (45) and (47) to deliver the same surface rotational velocity at $t=0$, provided that

$$\varphi'_\alpha(0)=\frac{\sin 2\varphi(0)}{2L}+l\varphi''_\alpha(0). \tag{50}$$

By inserting Eq. (49) into Eq. (50), this latter becomes an equation for α, which yields

$$\alpha=\frac{\xi[\sin 2\varphi(0)+2Ll\varphi'(0)]}{2L(2l+\xi)\varphi(0)}. \tag{51}$$

Thus Eq. (48) delivers an adapted initial profile φ_a which complies with the Derzhanski-Petrov boundary condition. The adaptation length ξ can be chosen so as to make φ_α the closest possible to φ: the shorter ξ, the smaller the deviation between φ_α and φ. For α as in Eq. (51), φ_α evolves according to Eqs. (45) and (47).

We solved these equations numerically for $\varphi\equiv\pi/4$ and different values of l and ξ. While varying ξ in the interval $[0,h]$ had almost no effect on the evolution of φ_α, the changes in l were detectable. Figure 6 illustrates the snapshots at $t=\tau_h$ from three different evolutions, namely, the one ruled by the dilution model and those corresponding to $l=0$ and h: relative to the first one, the surface evolution is quicker for $l=0$ and slower for $l=h$; in both cases $\xi=h/2$. Figure 7 shows a different view of the same comparison: here the surface orientation $\vartheta|_{z=0}$ is plotted as a function of time for the three different evolutions. The graph obtained from the dilution model is uniformly bounded between those of the adapted evolutions with $l=0$ and h; this suggests that choosing the surface length l in the interval $[0,h]$ would make the surface relaxation of the adapted initial profile agree with that of the nonadapted one. A similar computation was performed for the relaxation from equilibrium after removal of the field; for every $l\in[0,h]$ the surface relaxation of the adapted profile was almost indistinguishable from that of the nonadapted one.

This is an exact way of interpreting the Derzhanski-Petrov condition. Although it cannot be properly applied to all initial director profiles, it can be to the adapted ones. The comparison between the evolution of adapted and nonadapted profiles shows that the phenomenological surface length l hidden in the surface viscosity is indeed close to the length h over which the surface potential extends into the bulk.

VIII. CONCLUSIONS

We studied the relaxation of the anchoring of nematic liquid crystals close to a solid boundary. We employed a mathematical model where the orienting field at the interface between the liquid crystal and the solid substrate is not concentrated at the boundary, but is diluted over a small, though still macroscopic, layer with thickness h. We studied a model problem where the preferred orientation induced by the surface field is parallel to the boundary. The nematic orientation is distorted by an electric field orthogonal to the bounding plate. The equilibrium problem had already been treated in [12,14]. Here we attacked the dynamical problem that arises when an initial profile is allowed to relax freely. We considered two classes of initial profiles, namely, equilibrium profiles obtained by applying and then abruptly removing an electric field with strength below saturation, and flat profiles, possibly produced by combining fields above saturation and an applied shear flow, both suddenly removed. We wrote the

evolution equation for this problem, made analytical estimates for its main features, and computed its solutions numerically.

The main result of this paper is the dramatic difference in the relaxation dynamics following initial states in these classes. The evolution starting from equilibrium profiles after removal of the field follows adiabatically quasiequilibrium profiles corresponding to lower electric fields; the characteristic relaxation time is of the order $\tau_L = \gamma_1 L^2/K$ (or larger), which depends only on the total strength of the diluted surface potential $A = K/L$. In general L is smaller than the typical size of nematic cells, so that τ_L should be considered as a short time in standard nematodynamics. In this mode the relaxation is indeed controlled by the bulk, and the surface remains at equilibrium. The real surface relaxation mode, where most of the dissipation is localized near the boundary, corresponds to what is here called the fast mode; it is associated with the other class of initial profiles, whose characteristic time is found to be of the order of $\tau_s = \gamma_1 hL/K$. Since in the dilution model employed here $h \ll L$, then $\tau_s \ll \tau_L$. At later times, however, this fast mode is hampered by bulk diffusion and behaves as a slow mode.

In principle, it seems plausible to realize a flat initial profile by using an external field E_∞ that is extremely large and has suitable orientation. One could then argue that there is only one class of free relaxation problems to discuss, that is, those originating from profiles produced by a field: the relaxation mode with maximum amplitude should then correspond to the relaxation rate $1/\tau_\infty$ which diverges like E_∞^2. In fact, this is true as long as the coherence length ξ_e associated with the applied field E_∞ is larger than h: the curvature density present in the bulk before relaxation keeps memory of the field and determines a relaxation rate $1/\tau_e$. When, however, ξ_e is smaller than h, no memory of the field is left and the relaxation rate of the mode with maximum amplitude is $1/\tau_s$, associated now with the surface field, which reveals an intrinsic property of the anchoring.

We have evidence that these results are valid for a large range of parameters and different dilution laws, provided $h \ll L$. It could be useful to measure these relaxation processes, first to check the validity in dynamics of the dilution model, and then possibly to obtain information on the internal structure of the surface by comparing τ_s with τ_L.

For simplicity, we have not considered here the effective viscosity introduced in [12] to account for the backflow; actually, any flow has been neglected in the relaxation. We have numerical evidence that the reduction of viscosity due to backflow could slightly modify these results, but it would not change the difference between the slow and fast relaxation. This will be illustrated elsewhere.

The Derzhanski-Petrov dynamical boundary condition, which introduced the surface viscosity γ_s, has been widely accepted up to now because it seemed to convey a physical meaning: it was natural to derive a surface viscous torque from a localized surface dissipation. An important point made at the beginning of our work is the condition on the initial director profile required to make bulk and surface dynamics compatible. This compatibility restriction prevents the general use of the Derzhanski-Petrov boundary condition. We have developed a general strategy to adapt the initial profile so as to make this condition applicable. The interesting outcome of the comparison between this adapted evolution and the one predicted by the dilution model is that the surface length l hidden in γ_s turns out to be close to the thickness h of the layer where the surface potential is diluted into the bulk. With such a proper choice for the surface viscosity, the classical Derzhanski-Petrov model and the dilution model give comparable outcomes.

[1] I. Dozov, M. Nobili, and G. Durand, Appl. Phys. Lett. **70**, 1179 (1997).
[2] I. Dozov and G. Durand, Liq. Cryst. Today **8**, 1 (1998).
[3] A. Rapini, Can. J. Phys. **53**, 968 (1975).
[4] S. Pikin, G. Ryschenkow, and W. Urbach, J. Phys. (Paris) **37**, 241 (1976).
[5] A. I. Derzhanski and A. G. Petrov, Acta Phys. Pol. A **55**, 747 (1979).
[6] M. Kléman and S. A. Pikin, J. Mec. **18**, 661 (1979).
[7] A. D. Rey, Macromolecules **24**, 4450 (1991).
[8] A. Gharbi, F. R. Fekih, and G. Durand, Liq. Cryst. **12**, 515 (1992).
[9] J. Stelzer, R. Hirning, and H.-R. Trebin, J. Appl. Phys. **74**, 6046 (1993).
[10] P. J. Kedney and F. M. Leslie, Liq. Cryst. **24**, 613 (1998).
[11] J. G. McIntosh and F. M. Leslie, J. Eng. Math. **37**, 129 (2000).
[12] G. E. Durand and E. G. Virga, Phys. Rev. E **59**, 4137 (1999).
[13] E. Dubois-Violette and P. G. De Gennes, J. Colloid Interface Sci. **57**, 403 (1976).
[14] A. M. Sonnet and E. G. Virga, Phys. Rev. E **61**, 5401 (2000).
[15] P. G. De Gennes and J. Prost, *The Physics of Liquid Crystals*, 2nd ed. (Clarendon, Oxford, 1993).
[16] F. M. Leslie, Arch. Ration. Mech. Anal. **28**, 265 (1968).
[17] F. M. Leslie, Continuum Mech. Thermodyn. **4**, 167 (1992).
[18] A. Mertelj and M. Čopič, Phys. Rev. Lett. **81**, 5844 (1998).
[19] E. G. Virga (unpublished).